

NINETEENTH EUROPEAN ROTORCRAFT FORUM

Paper n° B3

HELICOPTER ROTOR NOISE PREDICTIONS
USING 3D COMPUTED AERODYNAMIC DATA
FOR DIFFERENT BLADE GEOMETRIES

by

C. Polacsek, J. Zibi, M. Costes

Office National d'Etudes et de Recherches Aérospatiales
Châtillon, France

September 14-16, 1993
Cernobbio (Como)
Italy

ASSOCIAZIONE INDUSTRIE AEROSPAZIALI
ASSOCIAZIONE ITALIANA DI AERONAUTICA ED ASTRONAUTICA

HELICOPTER ROTOR NOISE PREDICTIONS USING 3D COMPUTED AERODYNAMIC DATA FOR DIFFERENT BLADE GEOMETRIES

by C. Polacsek, J. Zibi, M. Costes
Office National d'Etudes et de Recherches Aérospatiales
BP 72, 92322 Châtillon Cedex, France

ABSTRACT

Acoustic calculations based on the Ffowcs Williams-Hawkings equation have been performed using the data given by a 3D full potential code. These methods have been applied to two four-bladed rotors, the 7A and the 7AD rotors, in order to estimate the theoretical noise reduction with respect to advanced blade tip geometry or reduced rotation speed.

Acoustic time signatures and sound pressure levels computed for several kinematic parameters are compared and correlated to the aerodynamic field in the vicinity of the blade, with a special emphasis on transonic flows. These predictions are also compared to experimental data obtained in the ONERA S1-Modane wind tunnel.

The noise reduction provided at high-speed by the 7AD parabolic tip is about 8 dB(A) in the rotor plane, in the advancing direction. Furthermore, a reduction of 5% on the rotor rotation speed brings about a 15 dB(A) noise reduction.

NOTATIONS

c	= Blade chord
C_d	= Drag coefficient
C_l	= Lift coefficient
C_p	= Local blade pressure coefficient
C_T/σ	= Rotor lift coefficient
M_p	= Advancing tip Mach number
$M_{\Omega R}$	= Rotation tip Mach number
R	= Rotor radius
T	= Period of the rotor revolution
V_0	= Advancing speed
μ	= Advance ratio
σ	= Blade solidity
Ψ	= Blade azimuth

ABBREVIATIONS

FP3D	: Unsteady Three Dimensional Full Potential Rotor Code.
HSI noise	: High Speed Impulsive noise.
PARIS	: Acoustic Prevision of a Rotor Interacting with its Wake.
SPL	: Sound Pressure Level.

1. INTRODUCTION

Helicopter noise reduction has been a constant trend for the two last decades. This effort is even becoming more critical in the present time. For civil applications, stronger limitations are

imposed by certification rules to reduce acoustic nuisance. Military helicopters are also concerned by noise reduction in order to limit their detectability. The development and validation of accurate prediction tools for helicopter aeroacoustics is therefore of great interest, since they will become essential during the design process. Experiment, which allows to understand the basic phenomena and to test new concepts, is a complementary aspect of research in this field. This paper deals with both theoretical and experimental aeroacoustics of helicopter rotors in high-speed forward flight.

Extension of the flight envelope of future helicopters towards higher advancing speeds comes up against the occurrence of high-speed impulsive noise. This problem is difficult to simulate from both the aerodynamic and acoustic points of view. The design of a "quiet helicopter rotor" makes it necessary to develop accurate tools for this part of the flight domain of the helicopter.

An aerodynamic code, FP3D, and an acoustic code, PARIS, were applied to compute the aeroacoustics of two modern rotors, the 7A and 7AD, which were tested in the ONERA S1-Modane wind tunnel. The main objectives of this work are:

- ☞ to quantify the acoustic radiation of each rotor in terms of thickness noise (monopole sources) and loading noise (dipole sources);
- ☞ to validate the aero-acoustic computations using experimental data;
- ☞ to qualitatively estimate the blade behavior with respect to HSI noise, by displaying the delocalization phenomenon on transonic flow simulations.

An assessment of the acoustic gains provided by the 7AD blade compared to the reference blade is made. The influence of a reduction of the rotation speed is also analysed.

2. PRESENTATION OF AERODYNAMIC AND ACOUSTIC CODES

2.1 Aerodynamic Codes

2.1.1 R85 and METAR Codes

The R85 code, developed by ECF, is a rotor performance code which trims the rotor by iteratively solving mechanical equations written for the blades to which aerodynamic and inertial stresses are applied. The blade aerodynamics is simulated by a quasi-steady lifting line analysis, for which blade section geometries are taken into account using 2D airfoil tables. The wake is discretized by vortex lattices of prescribed geometry (METAR, developed by ECF).

2.1.2 FP3D Code

The 3D Full Potential rotor code,¹ initially developed within a cooperation between US Army and ONERA, solves the unsteady three-dimensional potential equation around a helicopter rotor blade. The flow is assumed to be isentropic and irrotational, so that the equations in a Galilean coordinate system (X, Y, Z, T) are:

- ☞ the mass conservation equation

$$\rho_T + (\rho\phi_X)_X + (\rho\phi_Y)_Y + (\rho\phi_Z)_Z = 0$$

the Bernoulli equation

$$\rho = \left[1 + \frac{\gamma - 1}{2} \left(M_\infty^2 - 2\phi_T - \phi_X^2 - \phi_Y^2 - \phi_Z^2 \right) \right]^{\frac{1}{\gamma - 1}}$$

where ϕ is the velocity potential and ρ the density.

A fully implicit conservative scheme is obtained from density and flux linearization. The mass conservation equation is discretized by second order in space and first order in time finite differences.

For lifting calculations, the inflow must be provided by an external model, METAR in the present case.

From the velocity potential, this method computes the velocity and pressure fields around the blade used as input data for acoustics.

2.2 PARIS Code

PARIS² calculates in the time domain the noise radiated by a helicopter rotor using the Goldstein formulation.³ The acoustic field is given by the equation:

$$p(\vec{x}, t) = \int_{\tau} \int_A \rho V_n \frac{DG}{D\tau} dS d\tau + \int_{\tau} \int_A \frac{\partial G}{\partial y_i} f_i dS d\tau$$

- ☞ A is the integration surface,
- ☞ f_i are the components of the aerodynamic force exerted on the fluid by a blade surface element,
- ☞ G is the Green function of the problem,
- ☞ t is the reception time,
- ☞ τ is the emission time,
- ☞ x is the observer coordinate in the Galilean frame,
- ☞ y_i are the coordinates of a blade surface element dS,
- ☞ $V_n = \vec{V} \cdot \vec{n}$, where V is the free stream velocity of this element and n is the unit vector normal to the surface (positive outside).

The first integral corresponds to the thickness noise, and the second to the loading noise. The volume integral corresponding to the quadrupole sources is not calculated. Though hovering non lifting calculations of HSI noise have already been performed,⁴ evaluation of quadrupole terms is not convenient with such an approach. A new method based on a Kirchhoff formulation is presently being developed at ONERA, in order to compute total rotor noise in forward flight.

Thickness noise calculation requires the complete kinematics of the rotor (V_n). Loading noise can be calculated by two ways: a direct method, which simplifies the surface sources on the blade in a dipole distribution (sectional forces) applied on the quarter chord line (compact source calculation) and a more rigorous method (more expensive), using the local blade pressures predicted by a 3D aerodynamic code (non compact source calculations).

2.3 Use of Aerodynamic Data

The chart of the aero-acoustic computations is given in Figure 1. Initial data include rotor geometry and general kinematics. Pre-calculations provide flight controls and induced velocities (R85 + METAR codes) needed by FP3D. These pre-calculations provide the blade motion used for the thickness noise computation with PARIS. They also give the blade loads necessary for a compact source calculation of the loading noise, using predicted C_d and C_l . The local surface pressure coefficients (C_p) and local Mach number (M_l) given by FP3D are respectively used for the non compact source calculations of the loading noise with PARIS and for numerical flow simulations. These simulations are an efficient way to predict the occurrence and the intensity of HSI noise (since it cannot be computed yet), by analysing the delocalization phenomenon^{5,6} (see § 4.3).

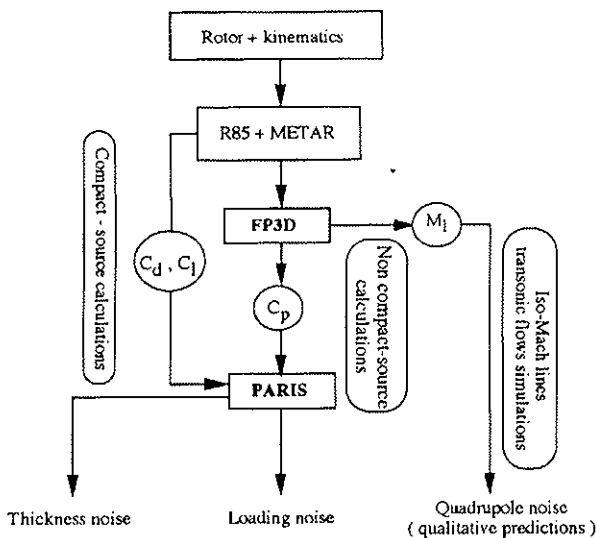


Figure 1
Aero-acoustic computation chart.

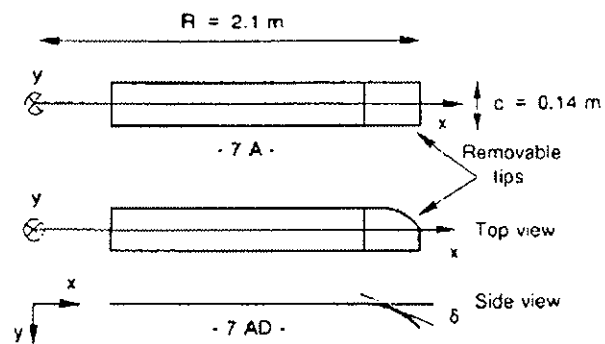


Figure 2
Blade planforms of the four-bladed rotor.

3 EXPERIMENTAL CONDITIONS

Blade geometry

The 7A and 7AD rotors are modern four-bladed rotors designed by ECF (Fig. 2). Both rotors are equipped with OA213 and OA209 airfoils and their only difference is the tip where the 7AD is fitted with a parabolic sweptback, SPP8 tip, while the 7A is rectangular.

Flight conditions

Flight parameters selected for computations on each rotor are:

$$M_{\Omega R} = 0.646 ; \mu = 0.3 \text{ and } \mu = 0.4 ; C_T/\sigma = 0.0625.$$

An additional point for the study of the influence of the rotation speed has been also computed on the 7A rotor:

$$M_{\Omega R} = 0.617 ; \mu = 0.4 ; C_T/\sigma = 0.0625.$$

Microphone locations

The locations of the two microphones used in S1-Modane for the 1991 wind tunnel tests⁷ are presented in Figure 3. Microphone 1 is located in the vicinity of the rotor plane (the rotor is tilted in forward flight), in the advancing direction. Microphone 2 is located below Microphone 1, under the rotor plane.

4. ACOUSTIC RESULTS

4.1 Comparisons between Compact Source and Non Compact Source Calculations

Compact source and non compact source calculations on the 7A rotor are presented in Figure 4 for the two microphones. The simplified method (using C_d and C_l) over estimates the predicted acoustic pressure, and the high-frequencies (small time scale fluctuations) are lost. This shows that 3D aerodynamic data are needed for accurate noise predictions. However, compact source calculations can give a fast estimate for rotor classification.

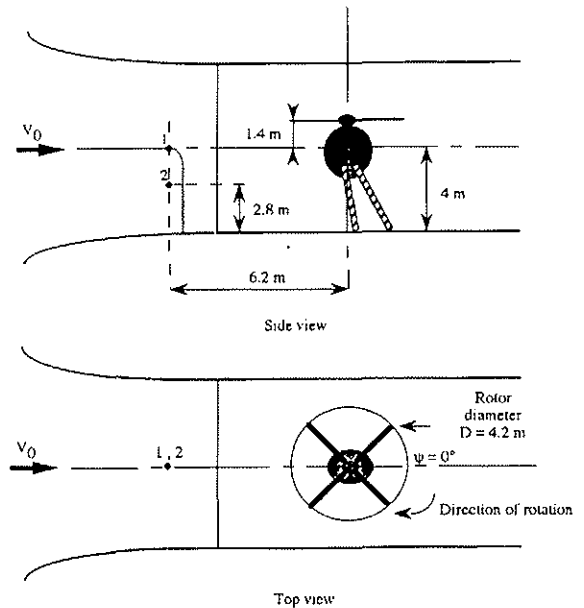


Figure 3
Microphone locations in S1-Modane wind tunnel.

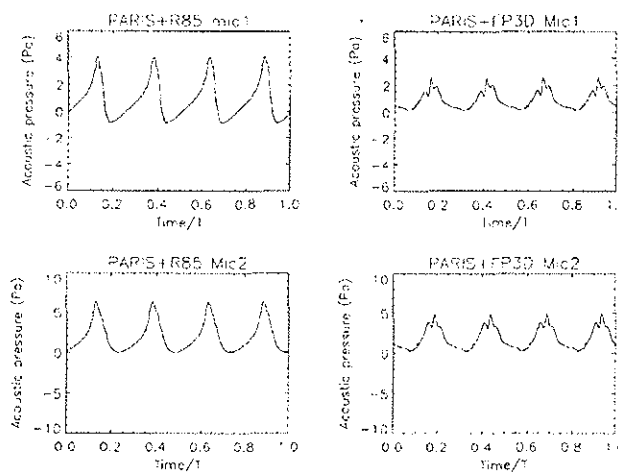


Figure 4
Comparisons between compact source and non compact source calculations.

4.2 Signatures and Noise Level Comparisons between 7A and 7AD Rotors

Computed acoustic signatures are presented in Figures 5 and 6, for each rotor and each flight condition, and at the location of Microphone 1.

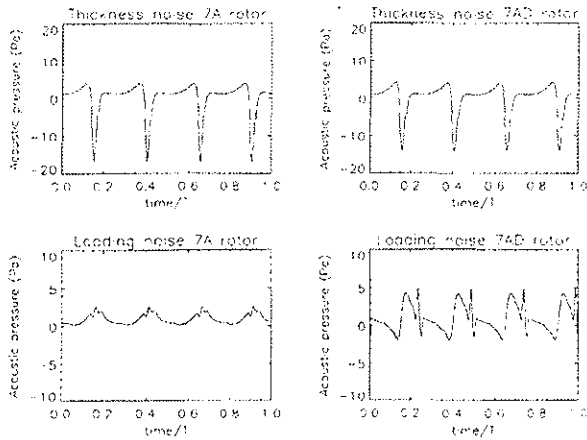


Figure 5
Comparisons of predicted acoustic signatures for 7A and 7AD rotors (non compact source calculations).
 $\mu = 0.3$; $M_{\Omega R} = 0.646$; $C_T/\sigma = 0.0625$.

At low speed ($M_p = 0.84$, Fig. 5), thickness noise radiated by 7AD rotor is slightly lower (about 2 dB(A)) than the one of the 7A rotor, which could be expected since the 7AD rotor is tapered in chord at the tip. However loading noise produced by the 7AD rotor is more intense and more impulsive (probably due to blade-vortex interactions). At high speed ($M_p = 0.9$, Fig. 6), the acoustic benefit obtained with the 7AD rotor for the thickness noise is emphasized. With respect to loading noise, the benefit provided by the 7AD blade is clearly noticeable (noise reduction of about 10 dB(A)). This loading noise reduction results from the decrease of the 7AD local blade pressure shown in Figure 7 (C_p , plotted versus chord position, are computed by FP3D on the upper surface of the blades at span station $r/R = 0.96$, and for $\Psi = 90^\circ$).

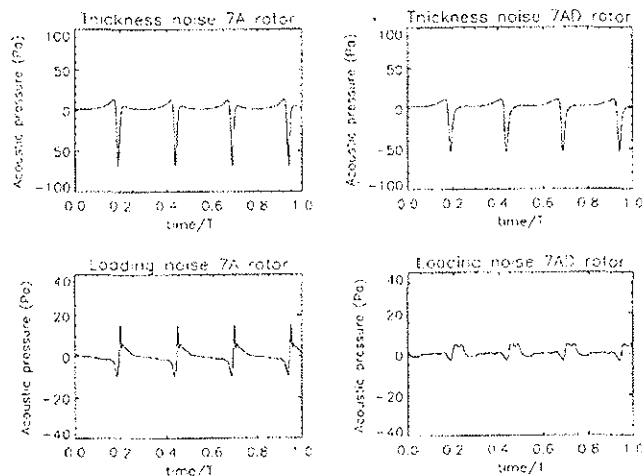


Figure 6
Comparisons of predicted acoustic signatures for 7A and 7AD rotors (non compact source calculations). $\mu = 0.4$; $M_{\Omega R} = 0.646$; $C_T/\sigma = 0.0625$.

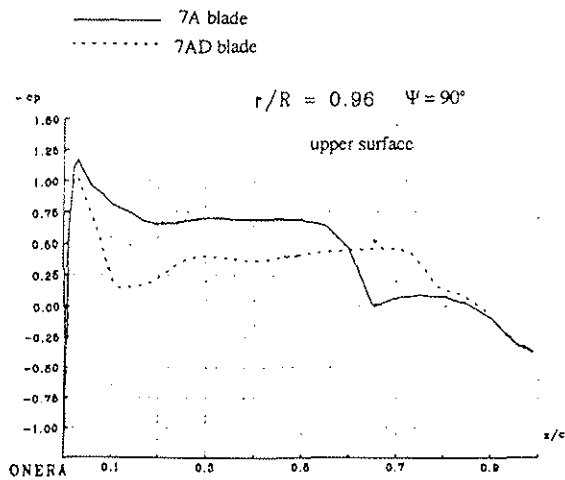


Figure 7
Local pressure distributions predicted by FP3D.
 $\mu = 0.4$; $M_{OR} = 0.646$; $C_T/\sigma = 0.0625$.

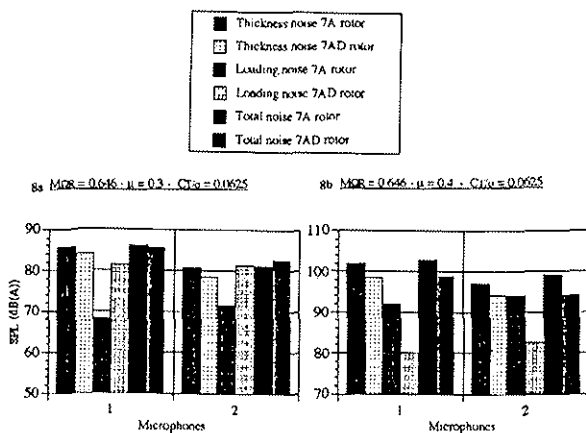


Figure 8
Predicted noise level comparisons.

Predicted dB(A) noise levels, calculated for a full-scale rotor, are summarized in Figure 8. "Total noise" in the figure refers to the sum of thickness and loading noise. At low speed (Fig. 8a), the total noise level predicted for the 7AD is equivalent (Microphone 1) or slightly higher (Microphone 2) than the 7A one due to the large loading noise contribution from the 7AD rotor. This result agrees with experimental SPL comparisons between 7A and 7AD rotors,⁷ showing that the 7AD rotor seems to be noisier than the 7A at low speed.

At high speed (Fig. 8b), the 7AD rotor total noise predictions (5 dB(A) reduction in SPL compared to the 7A rotor) confirm the acoustic interest of the blade tip geometry. In fact, present predictions do not include quadrupole noise, preponderant at high speed ($M_p 0.9$). The main advantage of 7AD compared to 7A, is a reduction of HSI noise due to lower transonic effects. This will be emphasized in the next section.

4.3 Transonic flow simulations

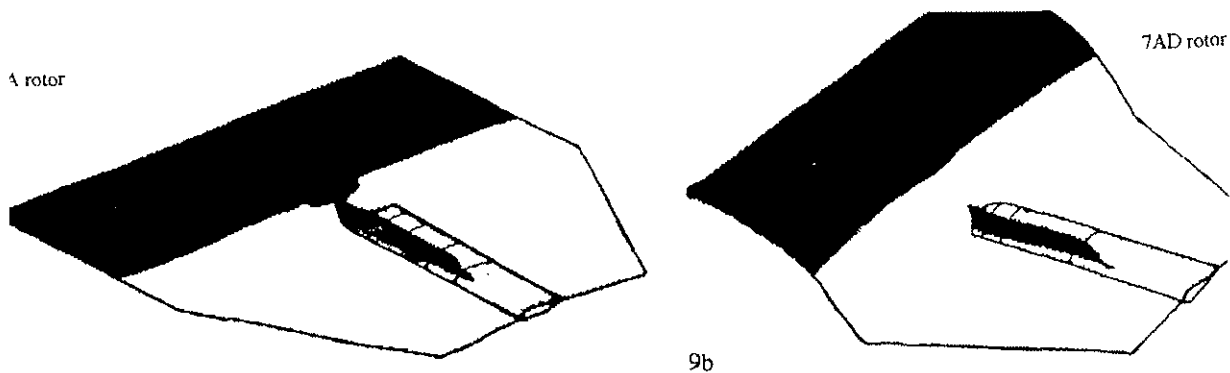
4.3.1 Influence of the Blade Planform

The local Mach numbers M_l computed by FP3D are used to generate iso-Mach maps on the blade upper surface grid from 0.5 R to 1.5 R. Figure 9 compares the transonic flows predicted at $\Psi = 90^\circ$ with the 7A blade (Fig. 9a) and the 7AD blade (Fig. 9b). The sonic cylinder is at 1.11 R and supersonic regions are dark colored.

In Figure 9a the delocalization phenomenon is clearly displayed: referring to the sonic line, inner and outer supersonic regions are connected. This allows for a shock radiation from the vicinity of the blade tip to the far field, in the upstream direction, causing intense impulsive noise.

In Figure 9b, the 7AD blade has not yet delocalized. This is due to a decrease of transonic effects by the blade tip planform.

Figures 9c and 9d compare the experimental acoustic signatures provided by Microphone 1 in S1-Modane for each rotor. The acoustic benefit obtained with the 7AD blade is about 8 dB(A).



Experimental acoustic signatures (S1-Modane)

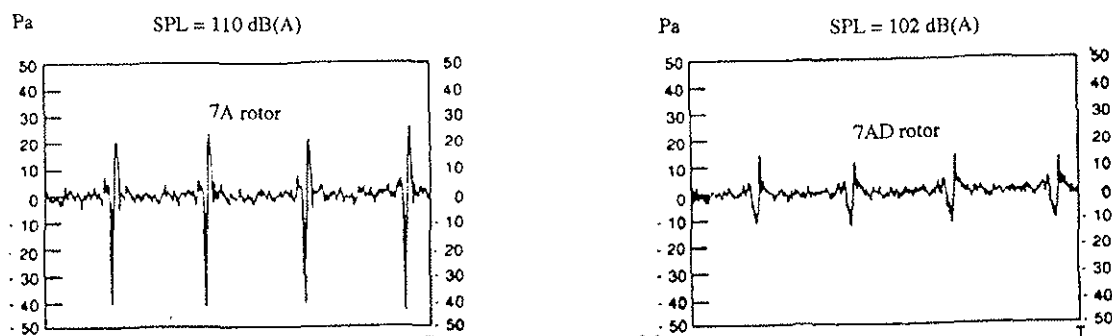


Figure 9
Reduction of transonic effects and correlation
with experimental data.

4.3.2 Influence of the rotation speed

Iso-Mach maps have been also generated for the 7A rotor at a lower rotation speed ($M_{\Omega R} = 0.617$ instead of $M_{\Omega R} = 0.646$), for the same flight conditions ($V_0 = 99$ m/s). The effect of a reduction of the rotation speed on delocalization is shown in Figure 10. Decreasing $M_{\Omega R}$ by only 5% produces a noise reduction of 15 dB(A) (Fig. 10a) due to the fact that delocalization does not occur at this lower rotation speed (see Fig. 10b).

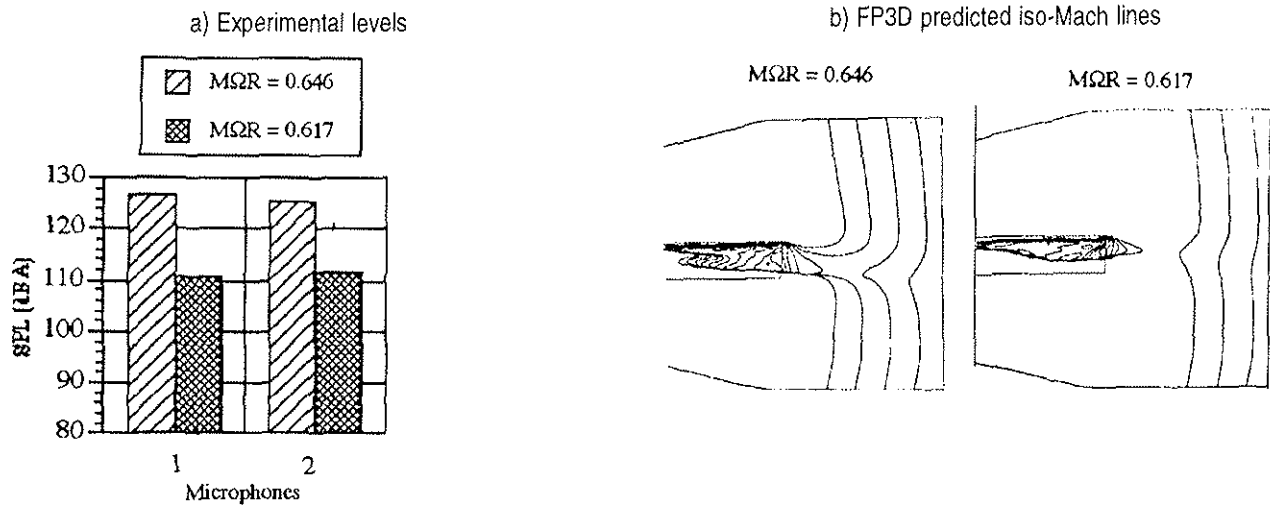


Figure 10
Benefit from a 5 % reduction of the rotation speed.

4.4 Correlations with experimental data

Correlations with experimental data are presented in Figures 11a and 11b, for the 7A rotor and Microphone 1. Computed noise is the sum of the thickness and the loading noise (no quadrupoles).

At $\mu = 0.3$ (Fig. 11a), contribution from quadrupoles (not calculated here) is negligible and theory/experiment comparison is quite good. The additional peaks and small fluctuations found in the experimental time signature are probably due to acoustic reflections which very much affect the low frequency components of the signal (the two first harmonics of the blade passage frequency, over-estimated in the experimental signature, have been numerically filtered).

At $\mu = 0.4$ (Fig. 11b), the steep recompression peak in the experimental signature corresponds to the shock which radiates in the far field because of 7A blade delocalization due to transonic effects (as seen in § IV.3.1). Consequently the difference between experiment and theory can be attributed to quadrupole contribution (monopole sources contribution towards negative pressure peak is about - 80 Pa).

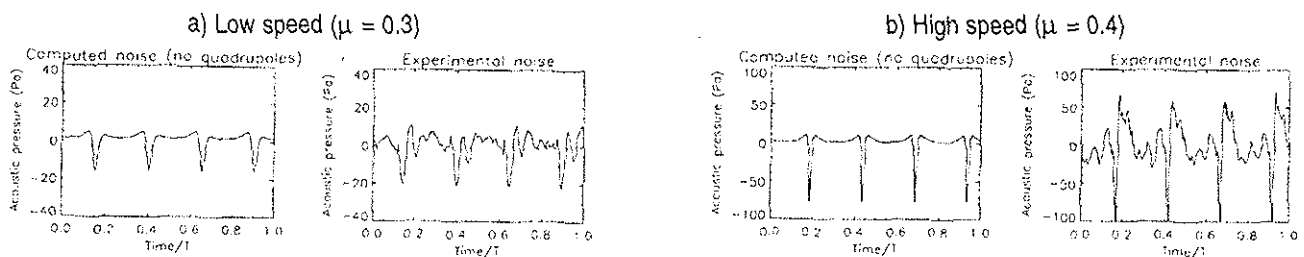


Figure 11
Comparisons between PARIS predictions and experimental results.

Comparisons made for the 7AD rotor (not presented here) lead to the same results.

4. CONCLUSION

A procedure to compute the aeroacoustics of helicopter rotors in forward flight has been presented. The aerodynamics is provided by an unsteady three dimensional analysis (FP3D), while the acoustics is computed by the Ffowcks Williams - Hawkings equation (PARIS). Quadrupole noise is not yet included in the computational procedure, which is therefore valid only at moderate high speed.

The method has been applied to two modern rotors (7A and 7AD) previously tested in the ONERA S1-Modane wind tunnel. Correlation between calculated thickness and loading noise and experiment shows a fairly good agreement as long as delocalization does not occur, while predicted noise is noticeably underestimated for higher speeds. Nevertheless, a good qualitative prediction of the behaviour of rotors with respect to HSI noise is provided by a pure aerodynamic criterion (delocalization criterion), as shown by correlation of noise measurements and transonic flow simulations.

It is found that an advanced tip geometry, such as the SPP8 tip, significantly delays delocalization by reducing transonic flows on the blade. A similar effect can also be obtained from a reduction in rotation speed.

In the future, a Kirchhoff formulation for quadrupole noise prediction, which is under development at ONERA, should be integrated in the computational procedure, giving then a tool suited to design a "quiet high-speed helicopter rotor".

REFERENCES

- 1 M. Costes, H.E. Jones, *Transonic Flow Potential Calculations on Helicopter Rotors*, 13th European Rotorcraft Forum, Arles, France, September 1987.
- 2 P. Spiegel, G. Rahier, B. Michea, *Blade-Vortex Interaction Noise: Prediction and Comparison with Flight and Wind Tunnel Tests*, 18th European Rotorcraft Forum, Avignon, France, September 15-18, 1992.
- 3 M.E. Goldstein, *Aeroacoustics*, McGraw Hill International Book Company, New-York, 1976.
- 4 J. Prieur, M. Costes, J. Baeder, *Aerodynamic and Acoustic Calculations of Transonic Nonlifting Hovering Rotors*, AHS Technical Specialists Meeting on Rotorcraft Acoustics, Philadelphia, October 15-16, 1991.
- 5 F.H. Schmitz, Y.H. Yu, *Transonic Rotor Noise Theoretical and Experimental Comparisons*, Vertica, Vol. 5, No. 1, pp 55-74, 1981.
- 6 J. Prieur, *Experimental Study of High-Speed Impulsive Rotor Noise in a Wind Tunnel*, 16th European Rotorcraft Forum, Glasgow, UK, September 1990.
- 7 C. Polacsek, P. Lafon, *High-Speed Impulsive Noise and Aerodynamic Results for Rectangular and Swept Rotor Blade Tip Tests in S1-Modane Wind Tunnel*, 17th European Rotorcraft Forum, Berlin, Germany, September 24-27, 1991.